

## Accepted Manuscript

Heavy Guadalquivir River discharge detection with satellite altimetry: the case of the eastern continental shelf of the Gulf of Cadiz (Iberian Peninsula)

J. Gómez-Enri, R. Escudier, A. Pascual, R. Mañanes

PII: S0273-1177(14)00815-1  
DOI: <http://dx.doi.org/10.1016/j.asr.2014.12.039>  
Reference: JASR 12087

To appear in: *Advances in Space Research*

Received Date: 8 June 2014  
Revised Date: 22 December 2014  
Accepted Date: 29 December 2014

Please cite this article as: Gómez-Enri, J., Escudier, R., Pascual, A., Mañanes, R., Heavy Guadalquivir River discharge detection with satellite altimetry: the case of the eastern continental shelf of the Gulf of Cadiz (Iberian Peninsula), *Advances in Space Research* (2015), doi: <http://dx.doi.org/10.1016/j.asr.2014.12.039>

This is a PDF file of an unedited manuscript that has been accepted for publication. As a service to our customers we are providing this early version of the manuscript. The manuscript will undergo copyediting, typesetting, and review of the resulting proof before it is published in its final form. Please note that during the production process errors may be discovered which could affect the content, and all legal disclaimers that apply to the journal pertain.



**Heavy Guadalquivir River discharge detection with satellite altimetry: the case of the eastern continental shelf of the Gulf of Cadiz (Iberian Peninsula)**

Gómez-Enri, J. (1)\*, Escudier, R. (2), Pascual, A. (2), and Mañanes, R. (1)

(1) Applied Physics Department. University of Cadiz (Spain).

(2) Instituto Mediterráneo de Estudios Avanzados (IMEDEA). CSIC-UIB (Spain).

ACCEPTED MANUSCRIPT

\*Corresponding author:

Jesús Gómez-Enri

jesus.gomez@uca.es

+34 956016071

**Abstract**

In-situ water levels in the Guadalquivir River estuary mouth show the effect of strong river freshwater discharges on the monthly means of the sea level in a yearly basis. Accurate altimeter products oriented to coastal zones are increasing the number of potential applications at different spatio-temporal scales. Present work is focused on the analysis of the sea level variability in the eastern shelf of the Gulf of Cadiz (between North Africa and the southwestern side of the Iberian Peninsula), adjacent to the Guadalquivir River estuary. Sixteen years (1994-2009) of along-track and standard AVISO maps of Sea Level Anomalies (SLA) have been used to generate a new high resolution product with increased spatio-temporal resolution. The use of a bathymetry constraint and smaller correlation scales in the methodology developed to generate high resolution altimeter products, improves the characterization of the mesoscale signals in the coastal strip adjacent to the estuary due to strong river freshwater discharges. This has been confirmed by the analysis of along-track SLA data in the vicinity of the estuary. The daily evolution (two weeks) of the sea level obtained in the event of December 2009 might be related to the river plume extension observed by optical Moderate Resolution Imaging Spectrometer (MODIS) images. The spatio-temporal distribution of the altimeter tracks available in the study area might compromise the mapping capabilities to capture coastal and fine-scale features.

Key words: coastal altimetry, sea level variability, river discharge, Gulf of Cadiz.

## 1. INTRODUCTION

Radar altimetry has become a powerful source of accurate sea level data in the open ocean (Fu and Cazenave, 2001), and more recently in the coastal fringe (Vignudelli et al., 2011). Indeed, coastal altimeter measurements have remained largely unexploited, due to several factors: wrong characterization of the geophysical corrections and inaccurate estimates of the distance between the satellite's centre of mass and the mean reflected surface (*range*), and Significant Wave Height (SWH). Near the shore the radar footprint might be contaminated by land and/or calm waters reflections complicating the retracking of radar waveforms, and hence the retrieval of the above mentioned parameters. Thus, Sea Level Anomalies (SLA) and SWH has had limited use near the coast. A number of initiatives have been made in the last decade to improve the accuracy and availability of altimeter data in the coastal zone. They are applied to along-track measurements (Vignudelli et al., 2005; Roblou et al., 2007; Brown, 2010; Liu et al., 2012), including the use of coastal-oriented corrections and the review of the data recovery strategies near the coast (Vignudelli et al., 2003; 2005; 2011; Bouffard et al., 2008a,b; 2010; 2012, Birol et al., 2010). In addition to this a better along-track spatial resolution (from 1 to 20 Hz) might improve the extraction of finer scales in coastal areas (Vignudelli et al., 2011). Alternatively, some innovative techniques for the generation of high-resolution (HR, henceforth) gridded maps of SLA have been developed by Dussurget et al. (2011) and Escudier et al. (2013). They made qualitative and quantitative comparisons with independent observations confirming that the new altimetry HR gridded products improve the characterization of coastal and fine-scale features. Thus, the number of applications exploiting accurate coastal altimeter reprocessed data has increased exponentially in the last years (Vignudelli et al., 2011, Pascual et al., 2013; Bouffard et al., 2014, among others).

Low-resolution (LR, hereinafter) ( $1/3^\circ \times 1/3^\circ$ ) gridded weekly maps of SLA routinely produced by AVISO (Archiving, Validation, and Interpretation of Satellite Oceanographic data, <http://www.aviso.oceanobs.com/>) have been used in the past to study the sea level variability over continental shelves at different time scales (Volkov et al., 2007; Saraceno et al., 2008; Gómez-Enri et al., 2012; Laiz et al., 2013; Caballero et al., 2014). In particular, Gómez-Enri et al. (2012) analyzed the effect of sporadic and heavy Guadalquivir river discharges in the sea level of the eastern continental shelf of

the Gulf of Cadiz. They concluded that these events could explain up to 50% of the variance of the daily mean sea level recorded by a tide gauge in the estuary mouth. Unexplained variance was found in the nearest LR altimeter point to the estuary (at 25 km to the mouth in the 50 m isobath). This could be indicating that the river runoff effect is restricted to the estuary mouth and along a small fringe near the coast. More recently, Laiz et al. (2013) demonstrated that LR weekly maps of SLA were unsuitable for the analysis of the Guadalquivir River sporadic discharges, due to the lack of altimeter data in the vicinity of the estuary mouth.

Nencioli et al. (2011) showed that LR maps could not resolve small and coastal features because of the smoothing applied to the data merging and interpolation. Dussurget et al. (2011) improved the temporal and spatial resolution of LR maps from weekly to daily and from  $1/3^\circ \times 1/3^\circ$  to  $1/16^\circ \times 1/16^\circ$  Mercator grid, respectively. They added the short scale signals to this HR product from the along-track data. More recently, Escudier et al. (2013) presented a new approach for the generation of HR maps of SLA that clearly improves the characterization of mesoscale signals in the coastal strip by adding a bathymetry constraint.

This work focuses on the capabilities of this new daily HR product (Escudier et al., 2013) to capture coastal and mesoscale processes. We present some examples of how these maps are able to show the daily evolution of a freshwater plume in the eastern continental shelf of the Gulf of Cadiz, after heavy discharges from the Guadalquivir River estuary. This has been confirmed by the analysis of the SLA signal observed in the altimeter tracks available in the vicinity of the estuary. The paper is organized as follows. We present in Section 2 the study area with Section 3 devoted to the data sets used (daily means of in-situ water levels, river discharges and altimeter-derived SLA) and methodology. The sea level response to heavy river discharges from daily to monthly time scales is analyzed using in-situ tide gauge data in the mouth of the Guadalquivir estuary. We then focus on two events of heavy freshwater river discharges (March 2001 – December 2009) analyzing the spatio-temporal distribution of the satellite SLA in the surrounding continental shelf of the river estuary mouth. We discuss the importance of the number and distribution of altimeter tracks in the study area during one strong event of river discharges (December 1996). The final remarks and conclusions are outlined in the last section.

## 2. STUDY AREA

The Gulf of Cadiz is located between North Africa and the southwestern side of the Iberian Peninsula. It connects the Atlantic Ocean with the Mediterranean Sea through the Strait of Gibraltar. Its continental shelf is located approximately within the 100 m isobath. It is divided in two halves by Cape Santa María: the western and eastern continental shelves. On the eastern side (Fig. 1) the Guadalquivir River, Tinto-Odiel system and Guadiana River are the main tributaries. The Guadalquivir River is the main contributor of freshwater discharge into the eastern shelf affecting the hydrology of the surrounding area (Prieto et al., 2009). The estuary has an extension of about 110 km between the mouth at Sanlúcar de Barrameda and the Alcalá del Río dam.

The river discharge has been identified as the main forcing agent of the hydrology inside the Guadalquivir estuary (Díez-Minguito et al., 2012; Navarro et al., 2012). Díez-Minguito et al. (2012) pointed out the lack of knowledge on the exchange of water masses between the continental shelf and the river. Several works have reported a strong decrease in salinity in the estuary mouth during episodes of strong river discharges (González-Ortegón and Drake, 2012; González-Ortegón et al., 2010; Navarro et al., 2012). This might indicate that the main effect in the adjacent continental shelf is an elevation of the sea level due to the less dense freshwater over the sea level. Prieto et al. (2009) analyzed the importance of heavy river discharges, together with the wind regime, in the triggering of phytoplankton growth on the shelf. In addition, the coastal warm surface counter-current flowing near the shore westward (spring-summer) and eastward (late autumn - early winter) over the eastern continental shelf (Stevenson, 1977; Relvas and Barton, 2002; García-Lafuente et al., 2006; Criado-Aldeanueva et al., 2009) could also be affected by these episodes. In summary, little is known about the sea level change in the adjacent eastern continental shelf due to heavy discharges of freshwater from the Guadalquivir River estuary.

## 3. DATA SETS AND METHODOLOGY

### 3.1 High-resolution maps of Sea Level Anomaly

Gridded LR weekly maps of SLA are generated by an optimal interpolation of the along-track data. These were obtained from AVISO with support from CNES (Centre National d'Études Spatiales). The gridded product used was the updated "Upd", which uses up to 4 altimeters (Ducet et al. 2000). This is a better choice than the reference "Ref" (only 2 altimeters) product for mapping the mesoscale variability (Pascual et al., 2006). The data quality of this product is ensured by the quality control process based on standard raw data editing (quality flags or parameter thresholds), including detection of erroneous artifacts and crossover validation (Aviso, 2014). From these, we generate 16 years of a new daily HR product (from January 1994 to December 2009) based on the methodology described in Escudier et al. (2013). A detailed description of the procedure to compute the HR maps of SLA used in this work is given in Escudier et al. (2013). A summary of the main steps is presented here. The procedure basically uses the capabilities of the LR maps and the along-track data to resolve the larger and finer scales, respectively. Firstly, prior to the optimal interpolation, the long-wavelength errors are removed from the along-track data using the mean of the LR maps linearly interpolated to the positions of the along-tracks (step 1). A daily map at a  $1/16^\circ \times 1/16^\circ$  regular grid is generated from the LR product by a temporal and spatial linear interpolation. This includes an optimal extrapolation near the coast using the Arhan function (Arhan and Colin de Verdiere, 1985), with a space correlation of 100 km, and a filter at 80 km to remove small scale features (step 2). The HR maps generated are linearly interpolated to the location of the tracks and subtracted to the along-track values (step 3). An optimal interpolation algorithm is then applied to the along-track residuals to generate daily fields of the finer scales (step 4). In this step, a bathymetry constraint can be taken into account in the interpolation process. The constraint is applied by modifying the correlation function and assuming a generalized distance that takes into account the topography (Davis, 1998; Escudier et al., 2013). The effect of the constraint results in giving more weight to observations that lies on the same bathymetric depth, inhibiting therefore sharp gradients across the coast. The topography used in this study has been extracted from Smith and Sandwell (1997). Finally (step 5), the smaller scales obtained in step 4 are added to the LR maps (containing the larger scales, step 2) to generate the final product fields (HR-std or HR-bathy if the bathymetry constraint is added).

### 3.2 Dynamic Atmospheric Correction

The static and dynamic ocean response to atmospheric forcing (pressure and wind) is modeled with the Dynamic Atmospheric Correction (DAC) developed by AVISO. The static correction basically accounts for the ocean response to low frequency atmospheric pressure variations assuming the isostatic assumption (Gil and Niiler 1973). The dynamic correction takes into account the high frequency pressure and wind signals (periods shorter than 20 days) using the MOG2D model (Carrère and Lyard, 2003; Pascual et al. 2008). Regular 6-hourly gridded maps of DAC (00:00, 06:00, 12:00, 18:00 GMT) were extracted from AVISO (<http://www.aviso.oceanobs.com/index.php?id=1278>).

### 3.3 Tide gauge data

Daily means of sea level heights covering the analyzed time period were obtained from the closest tide gauge station to the estuary mouth. It is a permanent station, moored in the port of Bonanza ( $37^{\circ}08'00''\text{N} - 6^{\circ}49'56''\text{W}$ ) at about 8 km to the mouth (Fig. 1). The instrument belongs to the Red de Mareografos (REDMAR) network of Puertos del Estado (Spain): <http://www.puertos.es>. The accuracy of the instrument is 2.5 mm with a resolution of 10 mm (ESEAS-RI, 2006). These data have been used in the past to validate LR weekly maps of SLA in the same area (Gómez-Enri et al., 2012; Laiz et al., 2013). These authors found a high level of agreement between both datasets at seasonal scales. Taking into account that the daily HR maps of gridded SLA are corrected by DAC, we estimated a daily mean DAC during the analyzed time period that was subtracted to the in-situ daily water levels in order to account for the atmospheric effects removed in the altimetry data set.

We analyzed the impact of heavy discharges on the water level in the river estuary mouth. We estimated monthly means of daily mean water levels (DAC corrected) from the tide gauge station at Bonanza (Fig. 1). We then obtained the average of the monthly means by averaging all the monthly mean water levels in January, February, etc. The lack of in-situ water level measurements in January (1997), March to June (1999), and November (2009) precluded the estimation of the monthly mean over these years.



### 3.4 River runoff

Daily means of flow rate ( $Q_d$  in  $\text{m}^3/\text{s}$ ) of the Guadalquivir River were obtained from the Automatic Hydrological Information System hosted by the Spanish Minister of Agriculture, Food and Environment (<http://www.chguadalquivir.es/saih>). We selected the nearest station to the estuary located at the Alcalá del Río dam (about 108 km upstream).

The mean  $Q_d$  in the time period analyzed was  $76.26 \text{ m}^3/\text{s}$ . The estuary is in normal conditions when  $Q_d$  is lower than  $40 \text{ m}^3/\text{s}$ , in extreme conditions for  $400 < Q_d < 3000 \text{ m}^3/\text{s}$ , and is catalogued as exceptional when  $Q_d > 3000 \text{ m}^3/\text{s}$  (Díez-Minguito et al., 2012). In normal conditions the estuary is tidally-dominated, with  $400 \text{ m}^3/\text{s}$  the limit for the river to be in a fluviially-dominated regime (Díez-Minguito et al., 2012; Navarro et al., 2012). Only 3.5% of the time period analyzed the river exceeded that value. We isolated 12 time periods with daily discharges higher than  $400 \text{ m}^3/\text{s}$  (extreme or exceptional conditions) during at least 3 days in order to avoid sporadic outflows due to regulation activities in the dam not related to heavy rain. Table 1 summarizes some information related to these periods (number of days with discharges higher than  $400 \text{ m}^3/\text{s}$ , maximum  $Q_d$  measured in that period and altimeter missions available during these periods). From the 12 heavy river discharges, 11 reached extreme conditions and only one (December 1996) was catalogued as exceptional. The twelve heavier discharges detected are presented in Table 1 and Fig. 2. The fluviially-dominated regime was achieved in autumn-winter seasons in all the cases. The longer periods of heavy  $Q_d$  were observed in 1997 (66 days), 1996 (54), 1998 (36), and 2001 (18). There is also a 4-years period of no heavy discharges between 2005 and 2008. This was also observed in 1994, 1995 and 2002. Thus, there is a decrease in the discharge with time in terms of amount of water and number of days. Navarro et al. (2012) analyzed a longer period of river discharges pointing out the decrease of the freshwater contribution to the estuary from  $5000 \text{ hm}^3/\text{year}$  (1931-1980) to  $2000 \text{ hm}^3/\text{year}$  (1981-2000). This reduction is greater during dry-year cycles. Discharges show a seasonal frequency and are driven by the regulation of the hydrographic basin upstream Alcalá del Río dam.

## 4. RESULTS AND DISCUSSION

We estimated the correlation coefficient between the monthly mean sea level of each year and the average of the monthly means (with the exception of the years with no monthly means available: 1997, 1999 and 2009). The correlations obtained were found not significant (95% confidence level for a p-value lower than 0.05) in the years of heaviest discharges (1996, 1998 and 2001). The highest significant correlations ( $p < 0.05$ ) were found in the years of negligible river discharges ranging between 0.92 (2007) and 0.64 (1995, 2000). We analyzed with more detail the year with the longer period of  $Q_d > 400 \text{ m}^3/\text{s}$  and maximum discharge (1996), and the year with the higher correlation (2007). Note that the estuary reached exceptional conditions ( $Q_d > 3000 \text{ m}^3/\text{s}$ ) in December 1996 (Table 1). Fig. 3a shows the monthly means in 1996, 2007 and the average of the monthly means for the whole time period. The monthly means during 2007 fits well to the average of the monthly means. In the extreme/exceptional conditions observed in 1996 strong discrepancies were found (January and December), making the correlation not significant ( $p < 0.05$ ). Fig. 3b gives the monthly mean river  $Q_d$  in 1996 and 2007 indicating that the deviations observed in the monthly means in 1996 are related to the monthly river discharges during these months. The same analysis was made in 1998 and 2001 (not shown) confirming these results. Thus, heavy freshwater discharges have a definite effect on the monthly means obtained in the estuary mouth during long periods of fluvial-dominated regime in the estuary.

The SLA obtained in the gridded maps is related to the along-track signals. The maps might be able to recover coastal and mesoscale signatures depending on the spatio-temporal distribution of the altimeter tracks in the area. That distribution is related to the available altimeter missions (Le Traon and Dibarboure, 2004; Pascual et al., 2006). We would expect a clear and distinctive signal in the along-track SLA data during strong discharges (Table 1) only if the satellites crossed the area close to the estuary, during those time periods. If so, these signals should be also observed in the HR-maps. To show this, we present in Fig. 4 Hovmöller diagrams with the along-track SLA. We used the closest tracks to the estuary during some of the heaviest discharges: ERS2 track #446 (January-February 1996 (1), December 1996 (2) and January-February 1997 (3) in Table 1), GFO track #046 (January 2001 (8) and March 2001 (9) in Table 1) and ENVISAT track #446 (December 2009 (12) in Table 1). The daily river discharge was also added. The along-track data clearly shows high SLA values during the time periods of heavy discharges (cases 1, 3, 8, 9 and 12 in Table 1). The increase in the sea

level seems to be confined to the coastal strip (25-30 km off the coast) where the influence of the river plume should be more important. During December 1996 (case 2) we do not observe high values of SLA in the track segment analyzed, because the satellite crossed the area eleven days before the tide gauge recorded the maximum water level.

We focus now on the analysis of the spatial distribution of the SLA using the high resolution maps. As mentioned, we analyze three events of heavy discharge: March 2001 (9) – December 2009 (12) and December 1996 (2).

#### 4.1 March 2001

We first focused on one time period in which the *Geosat Follow-On* (GFO) mission was operative (from January 2000 to September 2008). The reason for that was because this satellite presented the nearest track to the Guadalquivir estuary mouth (Fig. 1). From the 4 years of heavy discharges in that period we selected March 2001 as it showed the longer period of  $Q_d > 400 \text{ m}^3/\text{s}$  (15 days) and the highest amount of water discharge (up to  $2000 \text{ m}^3/\text{s}$ ). The analysis was made from 6<sup>th</sup> to 20<sup>th</sup> of March 2001. In that period the correlation coefficient between daily river discharge and in-situ water level was 0.70 ( $p < 0.05$ ). The comparison between HR-std (no bathymetry constraint added) and HR-bathy is presented in Fig. 5 in a temporal interval of 2 days. HR-std does not show significant geographical variations of SLA in any of the days analyzed. In the improved product, instead, there is a strong positive signal in the vicinity of the estuary mouth during about 8 days. The maximum was observed between March 12<sup>th</sup> and 14<sup>th</sup>. This signal could be related to the river discharges measured in that period, when the estuary was fluvially-dominated. The less dense freshwater plume should overlie the ocean water level increasing the sea level (Díez-Minguito et al., 2012). The improvement shown in HR-bathy is in agreement with a previous analysis in the northwestern Mediterranean Sea (Escudier et al., 2013). The authors focused on mesoscale dynamics showing an improvement in the spectral content in the HR-bathy, closer to the along-track signal, demonstrating that the inclusion of the bathymetry improves the capabilities of HR products to display higher levels of energy in the mesoscale bandwidth.

A detailed analysis of the event recorded in March 2001 is presented in Fig. 6. We compared the daily SLA between 1<sup>st</sup> and 20<sup>th</sup> of March obtained from the tide gauge at Bonanza (DAC correction applied), and the nearest altimeter point available in HR (std and bathy) (Fig. 6a): [36.8125°N, 6.4375°W] located at about 9 km to the station. The dates of the tracks available in the area and their geographical locations are also included. The mean daily  $Q_d$  is shown in Fig. 6b for comparison. The magnitude of the maximum SLA in the altimeter point selected is smaller than the water level measured in the tide gauge, and shows a delay of a few days. This delay might be explained by two factors: the spatio-temporal distribution of the tracks available in the area; and the temporal weighting applied to the along-track values of SLA used to generate the HR maps. To demonstrate this, Fig. 7 shows the along-track values of SLA when the satellites crossed the area between 09<sup>th</sup> and 16<sup>th</sup> of March. GFO #029 did not show high SLA probably because of the distance of the track to the eastern coast, and the fact that it was too early for the plume to be fully developed in the shelf near the estuary. One day after, the nearest track to the estuary mouth (GFO #046) showed the higher values of SLA (up to 15 cm) in the closest positions to the coast, confirming the effect of the heavy river discharge in the sea level measured by GFO. Due to the temporal scale of the interpolation that takes into account both GFO tracks, it does not appear in the 2D field. T/P #035 overpassed the zone six days later (15<sup>th</sup>) also showing high SLA near the coast. There, the interpolation uses this track and the GFO #046 to estimate the SLA. The bathymetry constraint applied helps in that regard because even if the segments of the two tracks close to the coast are far between them, they are at a similar bathymetry. Regarding the temporal weighting applied in the interpolations made to generate the maps, the along-track values of SLA are taken into account during 10 days from T-4d to T+5d, being T the dates and times of the measurements. Thus, we expect higher values of SLA in the HR maps between 10<sup>th</sup> and 15<sup>th</sup> of March considering GFO #046 and T/P #035 tracks. All these circumstances explain the date and position of the maximum observed in HR-bathy.

This illustration evidences the potential of using advances techniques for improving the spatio-temporal resolution of altimeter fields but, at the same time, highlights the need for higher temporal repetitiveness of the altimeter constellations, especially in the coastal areas.

#### 4.2 December 2009

Other sources of information in the area might be used to show the effect of the river discharge in the continental adjacent shelf. We analyze the event of December 2009 (Table 1) in terms of daily HR-bathy SLA maps and optical RGB MODIS (Moderate Resolution Imaging Spectrometer) images (Terra) available in AERONET (<http://lance-modis.eosdis.nasa.gov/imagery/subsets/?project=aeronet>). Water color might indicate the presence of high concentrations of sediment related to heavy discharges of freshwater from the river. The correlation between daily river discharge and water level (from 15<sup>th</sup> to 31<sup>st</sup>) was 0.77 ( $p < 0.05$ ). From the set of optical scenes in the study area we selected four days with cloud-free conditions. The RGB images and the corresponding maps of SLA are shown in Fig. 8. The river discharge started to be heavy after 22<sup>nd</sup> of December. Before that date the turbidity is scarce as shown in the optical images and the maps of SLA do not reflect any significant change in the vicinity of the estuary. A couple of days after that date the turbidity plume is clearly seen in the RGB images in the adjacent continental shelf reaching several hundred of km<sup>2</sup>. This is confirmed by the strong increase in SLA observed in HR-bathy. The water levels from the tide gauge at Bonanza (not shown here) confirmed this increase at that period. Navarro et al. (2012) analyzed this event in terms of temporal variability of some hydrological variables in the estuary (they expanded the analysis to March 2010). One of the stations was located in the estuary mouth recording routinely temperature, conductivity, dissolved oxygen, fluorescence and turbidity. The turbidimeter measured maximum values of about 8000 FNU (Formazin Nephelometric Unit) in that period. Salinity dropped to almost 0 confirming the freshwater nature of the plume in the estuary mouth.

#### 4.3 December 1996

The track coverage is not always optimal in the study area due to the lack of altimeter measurements during the episodes of heavy river discharges. As mentioned before, the best situation in terms of number and distribution of tracks was between January 2000 and September 2008 when the GFO data were available. In other periods it might be possible that the effects in the sea level due to heavy discharges are not observed in the daily maps of SLA just because of the scarcity of altimeter

measurements in the area at specific time periods. This is evident in the event of December 1996 (Table 1). During about the second half of the month, the river estuary was in extreme conditions with a fluviially-dominated regime ( $400 \text{ m}^3/\text{s} < Qd < 3000 \text{ m}^3/\text{s}$ ). Even though, the 24<sup>th</sup> of December the daily mean river discharge was  $3670 \text{ m}^3/\text{s}$ , making this event exceptional (Díez-Minguito et al., 2012). Under these conditions, one might expect a huge discharge of freshwater into the neighboring continental shelf and hence a clear and distinctive positive signal in the HR-bathy daily maps of SLA. The tide gauge confirmed an elevation of the mean daily water level of about 40 cm (not shown here) between 16<sup>th</sup> and 24<sup>th</sup> of December. The correlation coefficient between daily river discharge and water level in that period was 0.83 ( $p < 0.05$ ). Fig. 9 shows the HR-bathy daily maps of SLA from 16<sup>th</sup> to 31<sup>st</sup> of December. The river plume was not observed in any of the days shown. The track coverage during that period consisted of only one T/P track (#035) crossing the area twice (19<sup>th</sup> and 29<sup>th</sup> of December according to the temporal resolution of this satellite) in the southwestern corner of the selected area, and one ERS-2 track (#917) in the northwest (27<sup>th</sup> of December). Thus, the adjacent continental shelf to the estuary mouth was not covered by any altimeter passage and consequently the optimal interpolation used to generate the gridded maps was not capable to reproduce the expected increase of the sea level in the area.

## 5. SUMMARY AND CONCLUSIONS

Sixteen years (1994-2009) of sea level variability in the eastern continental shelf of the Gulf of Cadiz, adjacent to the Guadalquivir River estuary mouth, have been analyzed. We have focused on heavy events of freshwater discharges from the estuary and its influence on sea level at the adjacent shelf, ranging at temporal scales comprised between daily to monthly. Furthermore, the ability of high-resolution daily gridded maps of sea level anomaly generated from the constellation of radar altimeters available at that period capturing these events has been investigated in detail. From the results obtained in this work we outline the following conclusions:

In years with periods of heavy river discharges the monthly means of the sea level estimated in a yearly basis deviates from the average of the monthly means obtained along the whole time period. From the 9 years of strong discharges, 1996, 1998, 2001 and 2004 showed uncorrelated monthly means with the average of the

monthly means. Only 2000 and 2003 presented significant correlations. The lack of in-situ data in some years of heavy discharges precluded this comparison. The remaining years analyzed (no heavy discharges) showed significant and high correlations. We conclude that the sea level measured by the tide gauge close to the estuary mouth is highly influenced by sporadic but strong river discharges.

The use of a bathymetry constraint in the methodology developed to generate HR gridded maps of SLA (HR-bathy), improves the characterization of mesoscale signals in the coastal strip adjacent to the river estuary, respect to the standard product (HR-std). This has been demonstrated analyzing the spatio-temporal distribution of the SLA after two events of heavy river discharges of freshwater from the Guadalquivir River (March 2001 and December 2009). HR-bathy showed a more realistic elevation of the sea level in the vicinity of the estuary mouth, in agreement with in-situ observations and along-track SLA. The comparison against alternative remotely-sensed source (optical images) of information also confirms the extent of the freshwater plume in the adjacent shelf observed in the sea level maps.

The spatio-temporal distribution of the tracks covered by the satellite altimeter constellation is critical for the mapping capabilities of the HR maps to recover useful information. Any study area has to be covered by the maximum number of tracks in the space and temporal domains in order to get a more realistic characterization of the mesoscale signals.

## **ACKNOWLEDGMENTS**

This work has been partially supported by the ALCOVA Project (CTM2012-37839) funded by the Spanish Ministerio de Economía y Competitividad and FEDER. The low resolution maps of Sea Level Anomaly and along-track data were obtained from AVISO. Special thanks to Dr. Gabriel Navarro (ICMAN-CSIC) for his help on downloading and processing the MODIS-Terra RGB images from AERONET.



## REFERENCES

- Arhan, M., and A. Colin de Verdiere (1985). Dynamics of eddy motions in the eastern North Atlantic. *J. Phys. Oceanogr.* 15 (2), 153–170.
- Aviso (2014): SSALTO/DUACS User Handbook: (M)SLA and (M)ADT Near-Real Time and Delayed Time Products, CLS-DOS-NT-06-034 - Issue 4.1.
- Birol, F., M. Cancet, and C. Estournel (2010): Aspects of the seasonal variability of the Northern Current (NW Mediterranean Sea) observed by altimetry, *J. Mar. Syst.*, 81, p. 297–311. doi:10.1016/j.jmarsys.2010.01.005.
- Bouffard J., L. Renault, S. Ruiz, A. Pascual, C. Dufau, and J. Tintoré (2012): Sub-surface small scale eddy dynamics from multi-sensor observations and modelling, *Prog. in Oceanog.*, vol. 106. p.62-79.
- Bouffard J., S. Vignudelli, P. Cipollini, and Y. Ménard (2008b): Exploiting the potential of an improved multi-mission altimetric dataset over the coastal ocean. *Geophys. Res. Lett.*, 35, L10601, doi:10.1029/2008GL033488.
- Bouffard J., S. Vignudelli, M. Hermann, F. Lyard, P. Marsaleix, Y. Ménard, and P. Cipollini (2008a): Comparison of ocean dynamics with a regional circulation model and improved altimetry in the Northwestern Mediterranean. *Journal of Terrestrial, Atmospheric and Oceanic, sciences special issue "Satellite Altimetry over Land and Coastal Zones: Applications and Challenges"*, 19, No 1-2, 117-133, doi: 10.3319/TAO.2008.19.1-2.117(SA).
- Bouffard, J., A. Pascual, S. Ruiz, Y. Faugère, and J. Tintoré (2010): Coastal and mesoscale dynamics characterization using altimetry and gliders: A case study in the Balearic Sea, *J. Geophys. Res.*, 115, C10029, doi:10.1029/2009JC006087.
- Bouffard, J., F. Nencioli, R. Escudier, A. M. Doglioli, A.A. Petrenko, A. Pascual, P. M. Poulain, and D. Elhmaidi (2014): Lagrangian analysis of satellite-derived currents: Application to the North Western Mediterranean coastal dynamics, *Adv. in Space Res.*, 53, p. 788-801.
- Brown, S. (2010): A novel near-land radiometer wet path-delay retrieval algorithm: application to the Jason-2/OSTM Advanced Microwave Radiometer. *Trans. Geoc. Rem. Sens.*, doi: 10.1109/TGRS.2009.2037220.
- Caballero, A., L. Ferrer, A. Rubio, G. Charria, B. H. Taylor, and N. Grima (2014): Monitoring of a quasi-stationary eddy in the Bay of Biscay by means of satellite, *in-situ* and model results. *Deep Sea Res. Part II-Topical Studies in Oceanography*, doi: 10.1016/J.DSR2.2013.09.029.
- Carrère, L., and F. Lyard (2003): Modeling the barotropic response of the global ocean to atmospheric wind and pressure forcing - comparisons with observations. *Geophys. Res. Lett.* 30, 1275, doi: 10.1029/2002GL016473.
- Criado-Aldeanueva, F., J. García-Lafuente, G. Navarro, and J. Ruíz (2009): Seasonal and interannual variability of the surface circulation in the eastern Gulf of Cadiz (SW Iberia). *J. Geophys. Res.* 114, C01011, doi: 10.1029/2008JC005069.
- Díez-Minguito, M., A. Baquerizo, M. Ortega-Sánchez, G. Navarro, and M. A. Losada



- (2012): Tide transformation in the Guadalquivir estuary (SW Spain) and process-based zonation. *J. Geophys. Res.* 117, C03019, doi: 10.1029/2011JC007344.
- Ducet, N., P.-Y. Le Traon, and G. Reverdin, (2000): Global high resolution mapping of ocean circulation from *Topex/Poseidon* and *ERS-1* and *-2*. *J. Geophys. Res.*, 105 (C8), 19477-19498.
- Dussurget, R., F. Birol, R. Morrow, and P. De Mey (2011): Fine resolution altimetry data for a regional application in the Bay of Biscay, *Mar. Geod.*, 34, 3–4, 447–476, doi: 10.1080/01490419.2011.584835.
- Escudier, R., J. Bouffard, A. Pascual, P. M. Poulain, and M. I. Pujol (2013): Improvement of coastal and mesoscale observation from space: Application to the northwestern Mediterranean Sea, *Geophys. Res. Lett.* 40, 2148-2153, doi: [10.1002/grl.50324](https://doi.org/10.1002/grl.50324).
- ESEAS-RI, (2006): Assessment of accuracy and operational properties of different tide gauge sensors. WP4. Deliverable D4.1. European Sea-level Service Research & Infrastructure. 34 pp.
- Fu, L. L., and A. Cazenave (2001): *Satellite Altimetry and Earth Sciences: A handbook of Techniques and Application*, Academic Press, International Geophysics Series, Vol. 69, San Diego, USA, 463 pp.
- García-Lafuente, J., J. Delgado, F. Criado-Aldeanueva, M. Bruno, J. del Rio, and J. M. Vargas (2006): Water mass circulation on the continental shelf of the Gulf of Cadiz. *Deep Sea Res. Part II-Topical Studies in Oceanography* 53, 1182-1197, doi: 10.1016/J.DSR2.2006.04.011.
- Gill, A.E., and P. P. Niller (1973): The theory of the seasonal variability in the ocean. *Deep Sea Res. and Oceanographic Abstracts* 20, 141-177, doi: 10.1016/0011-7471(73)90049-1.
- Gómez-Enri, J., A. Aboitiz, B. Tejedor, and P. Villares (2012): Seasonal and interannual variability in the Gulf of Cadiz: Validation of gridded altimeter products. *Est. Coast. and Shelf Sci.* 96, 114-121, doi: 10.1016/J.ECSS.2011.10.013.
- González-Ortegón, E., and P. Drake (2012): Effects of freshwater inputs on the lower trophic levels of a temperate estuary: physical, physiological or trophic forcing? *Aq. Sci.* 74, 455-469, doi: 10.1007/S00027-011-0240-5.
- González-Ortegón, E., M. D. Subida, J. A. Cuesta, A. M. Arias, C. Fernández-Delgado, and P. Drake (2010): The impact of extreme turbidity events on the nursery function of a temperate European estuary with regulated freshwater inflow. *Est., Coast. and Shelf Sci.* 87, 311-324, doi: 10.1016/J.ECSS.2010.01.013.
- Laiz, I., J. Gómez-Enri, B. Tejedor, A. Aboitiz, and P. Villares (2013): Seasonal sea level variations in the gulf of Cadiz continental shelf from in-situ measurements and satellite altimetry. *Cont. Shelf Res.*, 53, 77-88, doi: 10.1016/J.CSR.2012.12.008.

- Le Traon, P. Y., and G. Dibarboure (2004): An illustration of the unique contribution of the TOPEX/Poseidon – Jason-1 tandem mission to mesoscale variability studies, *Mar. Geod.*, 27, 3–13
- Liu, Y., R. H. Weisberg, S. Vignudelli, L. Roblou, and C. R. Merz (2012): Comparison of the X-TRACK altimetry estimated currents with moored ADCP and HF radar observations on the West Florida Shelf. *Adv. Spac. Res.*, 50, 1085-1098, doi: 10.1016/J.ASR.2011.09.012.
- Navarro, G., I.E. Huertas, E. Costas, S. Flecha, M. Díez-Minguito, I. Caballero, V. López-Rodas, L. Prieto, and J. Ruiz (2012): Use of a real-time remote monitoring Network (RTRM) to characterize the Guadalquivir estuary (Spain), *Sensors* 12, 1398-1421, doi: 10.3390/S120201398.
- Nencioli, F., F. d'Ovidio, A. M. Doglioli, and A. A. Petrenko (2011): Surface coastal circulation patterns by in-situ detection of Lagrangian coherent structures, *Geophys. Res. Lett.*, 38, L17604, doi: 10.1029/2011GL048815.
- Pascual, A., Y. Faugère, G. Larnicol, and P. Y. Le Traon (2006): Improved description of the ocean mesoscale variability by combining four satellite altimeters, *Geophys. Res. Lett.*, 33, doi: 200610.1029/2005GL024633.
- Pascual, A., M. Marcos, and D. Gomis (2008): Comparing the sea level response to pressure and wind forcing of two barotropic models: Validation with tide gauge and altimetry data, *J. Geophys. Res.*, 113, doi: 10.1029/2007JC004459.
- Pascual, A., J. Bouffard, S. Ruiz, B. B. Nardelli, E. Vidal-Vijande, R. Escudier, J. M. Sayol, and A. Orfila (2013): Recent improvements in mesoscale characterization of the western Mediterranean Sea: Synergy between satellite altimetry and other observational approaches, *Scientia Mar.* 77, 19-36. doi:10.3989/scimar.03740.15A
- Prieto, L., G. Navarro, S. Rodríguez-Gálvez, I. E. Huertas, J. M. Naranjo, and J. Ruiz (2009): Meteorological and oceanographic forcing on the pelagic ecosystem of the Gulf of Cadiz shelf (SW Iberian Peninsula). *Cont. Shelf Res.*, 29, 2122–2137.
- Relvas, P., and E. D. Barton (2002): Mesoscale patterns in the Cape San Vicente (Iberian Peninsula) upwelling region. *J. Geophys. Res.* 107 (C10), 3164.
- Roblou, L., F. Lyard, M. Le Henaff, and C. Maraldi (2007): X-track, a new processing tool for altimetry in coastal oceans, in: ESA ENVISAT Symposium, Montreux, Switzerland, April 23–27, 2007, ESA SP-636.
- Saraceno, M., P. T. Strub, and P. M. Kosro (2008): Estimates of sea surface height and near-surface alongshore coastal currents from combinations of altimeters and tide gauge, *J. Geophys. Res.*, 113, C11013, doi: 10.1029/2008JC004756.
- Smith, W. H. F., and D. T. Sandwell (1997): Global sea floor topography from satellite altimetry and ship depth soundings, *Science*, 277(5334), 1956–1962.
- Stevenson, R.E., (1977): Huelva Front and Malaga, Spain, Eddy chain as defined by satellite and oceanographic data. *Deutsche Hydrographische Zeitschrift* 30 (2),

51–53.

Vignudelli S., P. Cipollini, F. Reseghetti, G. Fusco, G. P. Gasparini, and G. M. R. Manzella (2003): Comparison between XBT data and TOPEX/Poseidon satellite altimetry in the Ligurian-Tyrrhenian area. *Ann. Geophys.*, 21(1, Part 1), 123-135.

Vignudelli S., P. Cipollini, L. Roblou, F. Lyard, G. P. Gasparini, G. M. R. Manzella, and M. Astraldi (2005): Improved satellite altimetry in coastal systems: Case study of the Corsica Channel (Mediterranean Sea). *Geophys. Res. Lett.*, 32, L07608, doi:1029/2005GL22602.

Vignudelli, S., A. Kostianoy, P. Cipollini, and J. Benveniste (eds.) (2011): Coastal Altimetry, Springer, 1st Edition, 2011, XII, 566 p. 216 illus., 186 in color. doi: 10.1007/978-3-642-12796-0.

Volkov, D. L., D. L. Larnicol, and J. Dorandeu (2007): Improving the quality of satellite altimetry data over continental shelves. *J. Geophys. Res.*, 112, C06020, doi: 101029/2006JC003765.

**FIGURE CAPTIONS**

Figure 1. Study area with the location of the tide gauge (red star: Bonanza) and altimeter tracks used for the optimal interpolation analysis. Yellow dot indicates the position of the nearest altimeter grid point to the tide gauge.

Figure 2. Daily Guadalquivir River discharge (in  $\text{m}^3/\text{s}$ ) from January 1994 to December 2009. The numbers in parenthesis indicate the heavy river discharges shown in Table 1. An overview of the altimetry missions used is also shown.

Figure 3. Average of monthly means of Mean Sea Level (black line), monthly means (MSL) in 1996 (grey line) and in 2007 (dashed black line) (Fig. 3a). The monthly Mean River Discharge (MRD) in 1996 (grey line) and 2007 (solid black line) is shown in Fig. 3b.

Figure 4. Hovmöller diagrams of along-track SLA during some events of heavy discharge using the closest tracks available to the estuary. January-February 1996 (Fig. 4.a), December 1996 and January-February 1997 (Fig. 4.b), January-March 2001 (Fig. 4.c) and December 2009 (Fig. 4.d). The daily river discharge is also included.

Figure 5. Daily maps of SLA in a 2-days temporal interval in the study area between 6<sup>th</sup> and 20<sup>th</sup> March 2001 using HR-std (Fig. 5a) and HR-bathy (Fig. 5b).

Figure 6. Top: Daily sea level anomaly (DAC corrected) from the tide gauge (black line) from the closest grid point of HR-bathy (grey line) and HR-std (dashed black line) between 1<sup>st</sup> and 20<sup>th</sup> of March 2001. Also included the temporal location of the closest tracks to the Guadalquivir estuary. Bottom: Daily river discharge at the same period. The geographical location of the tracks available in the area for that period (ERS-2, GFO and Topex/Poseidon) are shown in the upper right corner of the bottom panel.

Figure 7. Along-track values of SLA (1 Hz sampling rate) for the constellation of satellites crossing the area between 09<sup>th</sup> and 15<sup>th</sup> of March 2001.

Figure 8. Left panel: RGB MODIS Terra images acquired in several dates during December 2009. Right panel: corresponding HR-bathy maps of SLA.

Figure 9. Daily maps of HR-bathy SLA from 16<sup>th</sup> to 31<sup>st</sup> December 1996.

ACCEPTED MANUSCRIPT

FIGURE 1

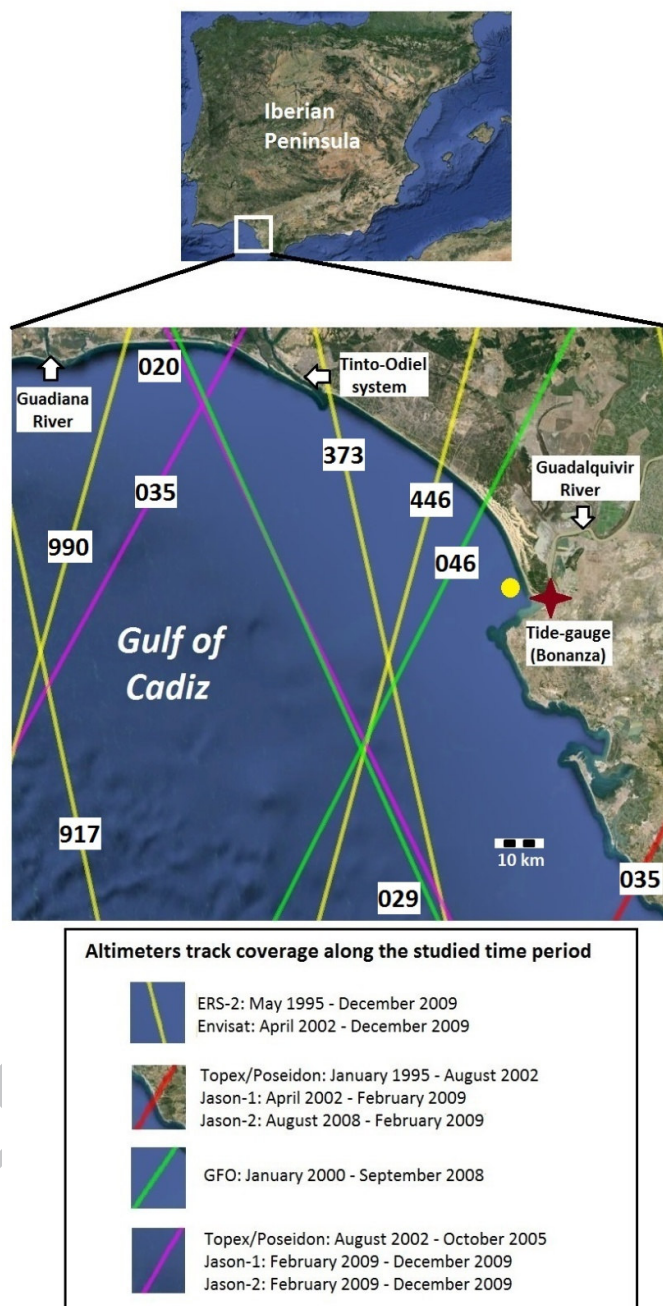


Figure 1. Study area with the location of the tide gauge (red star: Bonanza) and altimeter tracks used for the optimal interpolation analysis. Yellow dot indicates the position of the nearest altimeter grid point to the tide gauge.

FIGURE 2

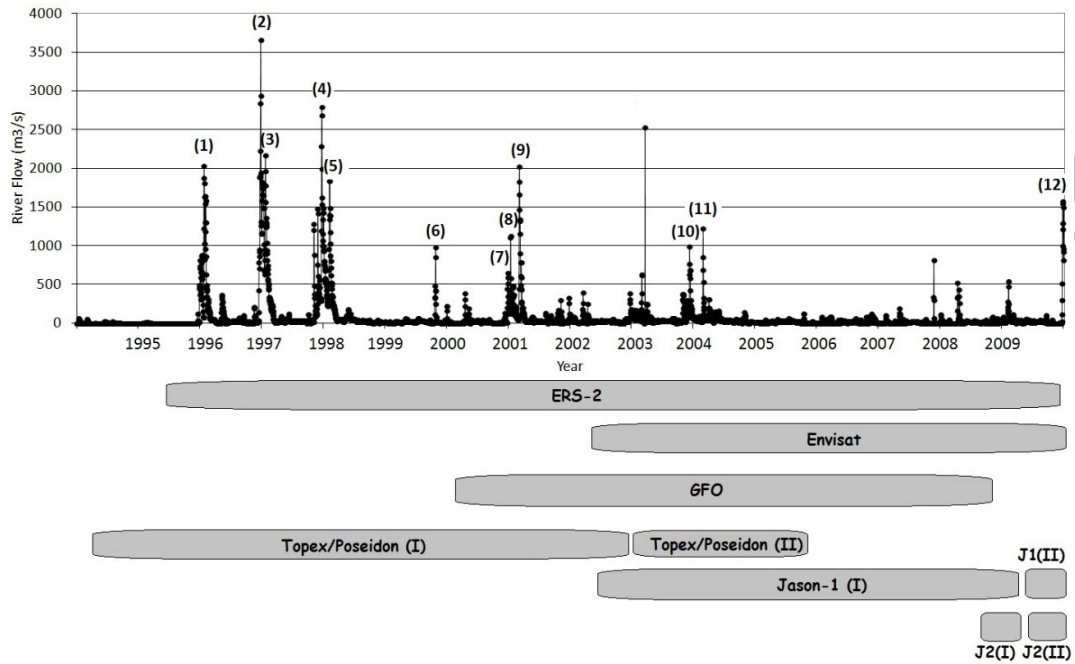


Figure 2. Daily Guadalquivir River discharge (in m<sup>3</sup>/s) from January 1994 to December 2009. The numbers in parenthesis indicate the heavy river discharges shown in Table 1. An overview of the altimetry missions used is also shown.

FIGURE 3

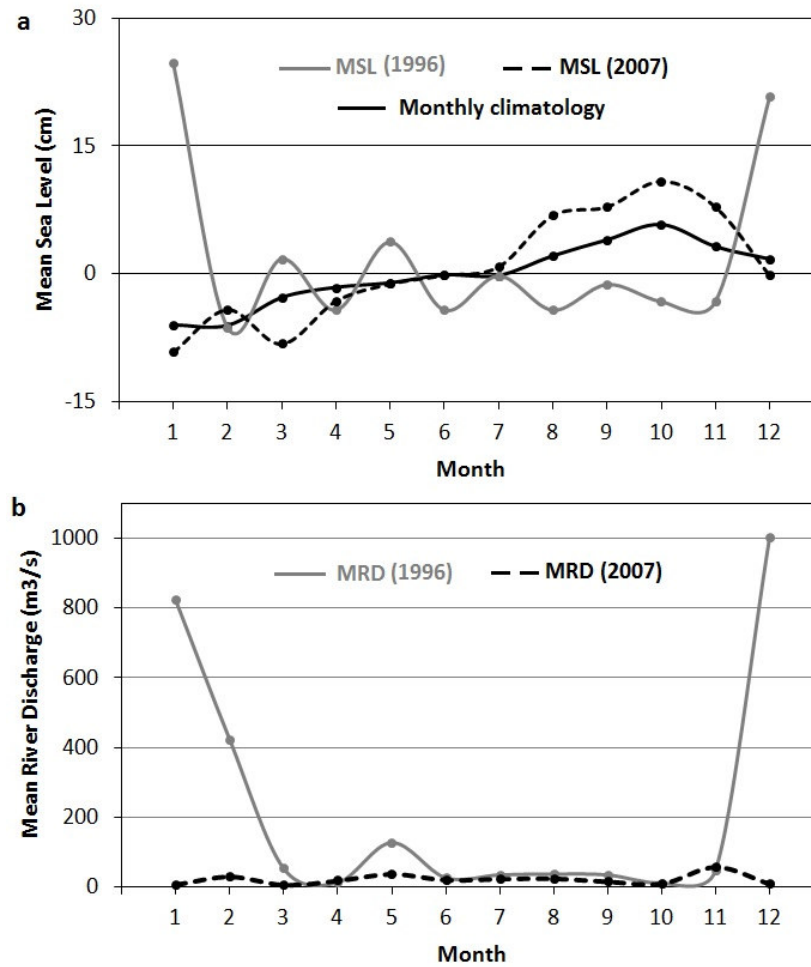


Figure 3. Average of monthly means of Mean Sea Level (black line), monthly means (MSL) in 1996 (grey line) and in 2007 (dashed black line) (Fig. 3a). The monthly Mean River Discharge (MRD) in 1996 (grey line) and 2007 (solid black line) is shown in Fig. 3b.



FIGURE 4

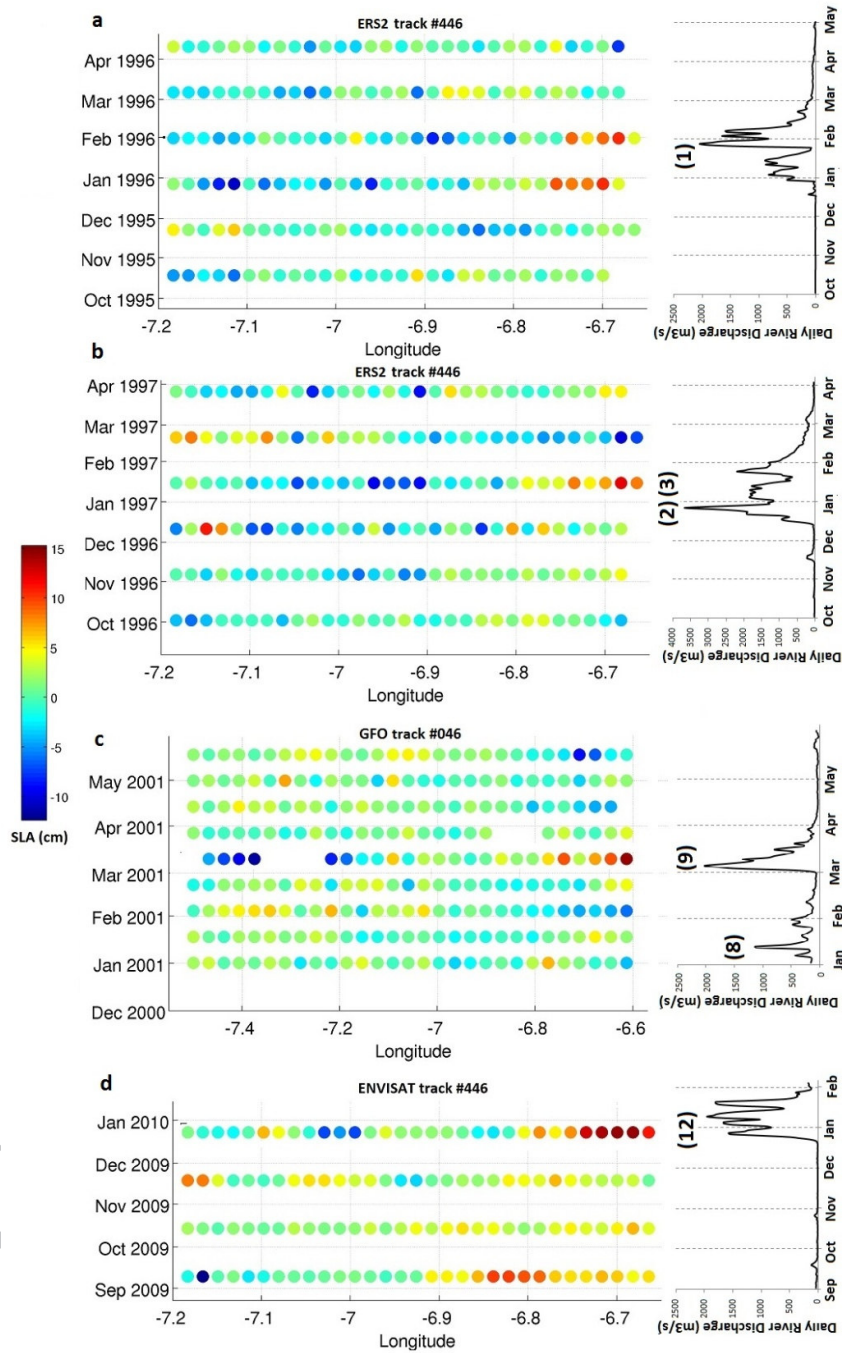


Figure 4. Hovmöller diagrams of along-track SLA during some events of heavy discharge using the closest tracks available to the estuary. January-February 1996 (Fig. 4.a), December 1996 and January-February 1997 (Fig. 4.b), January-March 2001 (Fig. 4.c) and December 2009 (Fig. 4.d). The daily river discharge is also included.

FIGURE 5

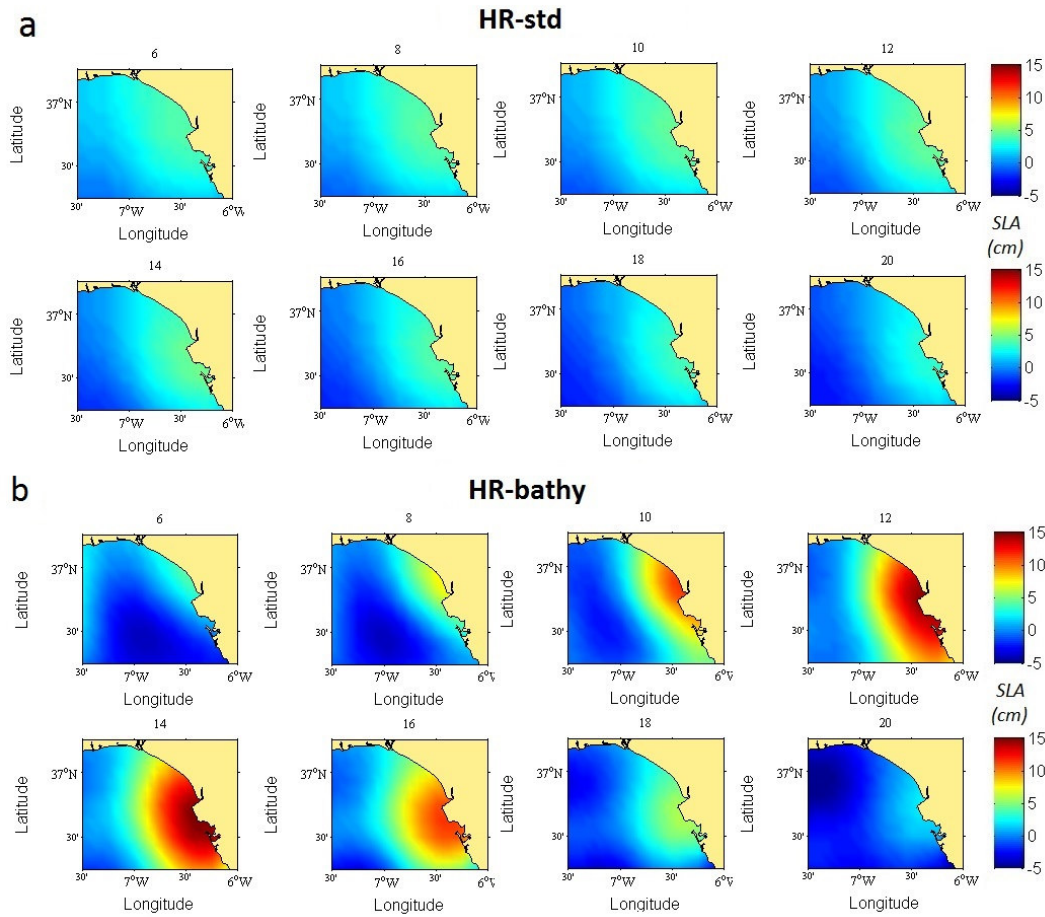


Figure 5. Daily maps of SLA in a 2-days temporal interval in the study area between 6<sup>th</sup> and 20<sup>th</sup> March 2001 using HR-std (Fig. 5a) and HR-bathy (Fig. 5b).

FIGURE 6

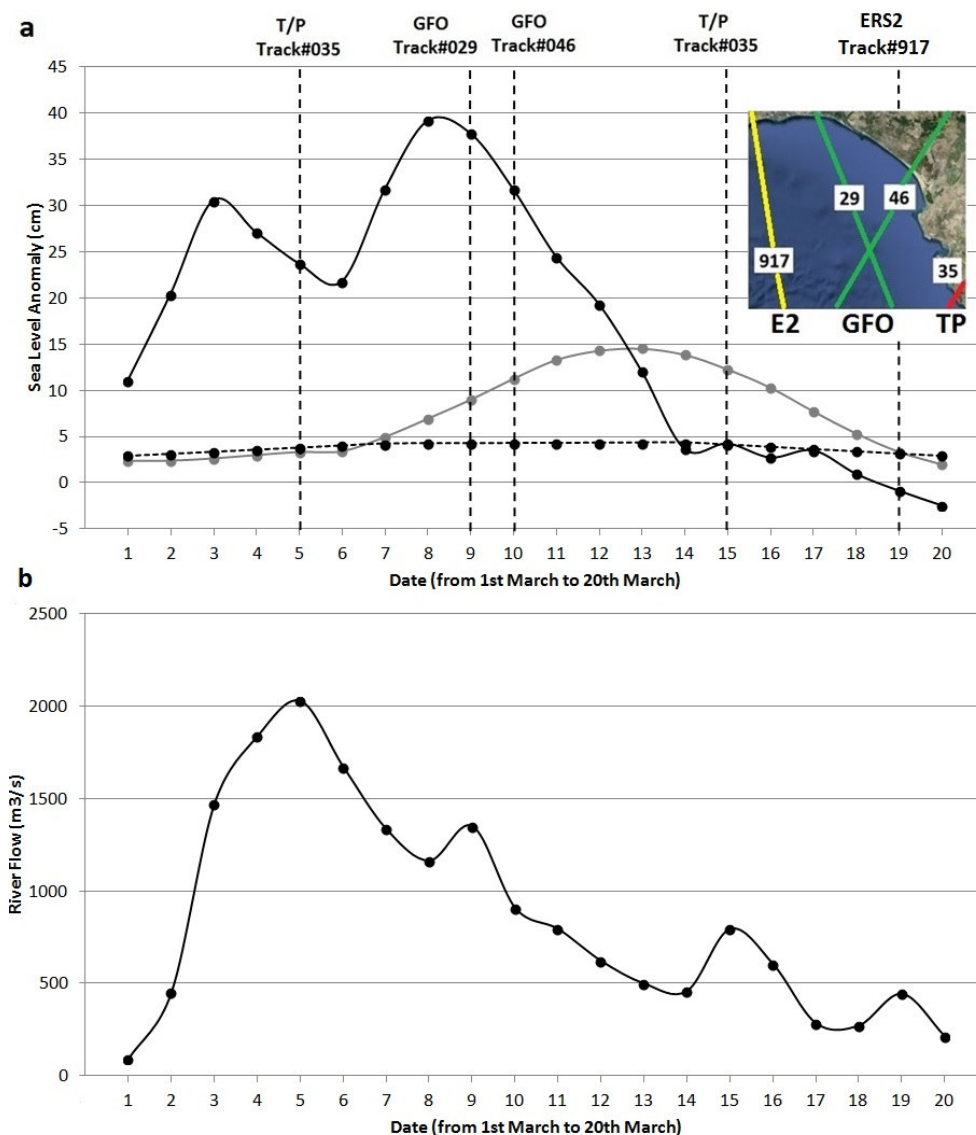


Figure 6. Top: Daily sea level anomaly (DAC corrected) from the tide gauge (black line) from the closest grid point of HR-bathy (grey line) and HR-std (dashed black line) between 1<sup>st</sup> and 20<sup>th</sup> of March 2001. Also included the temporal location of the closest tracks to the Guadalquivir estuary. Bottom: Daily river discharge at the same period. The geographical location of the tracks available in the area for that period (ERS-2, GFO and Topex/Poseidon) are shown in the upper right corner of the bottom panel.

FIGURE 7

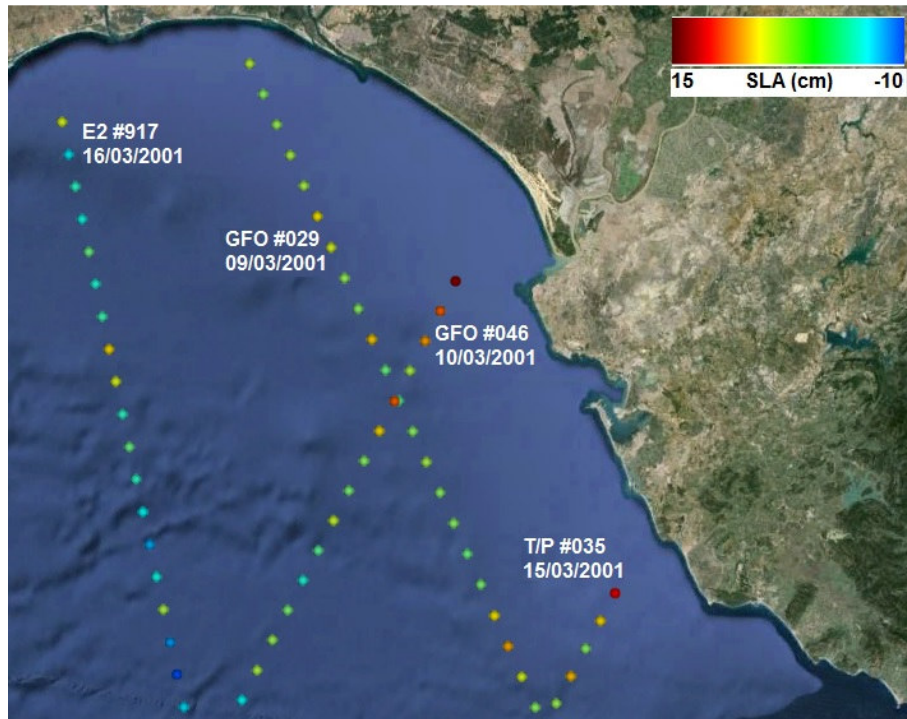


Figure 7. Along-track values of SLA (1 Hz sampling rate) for the constellation of satellites crossing the area between 09<sup>th</sup> and 15<sup>th</sup> of March 2001.



FIGURE 8

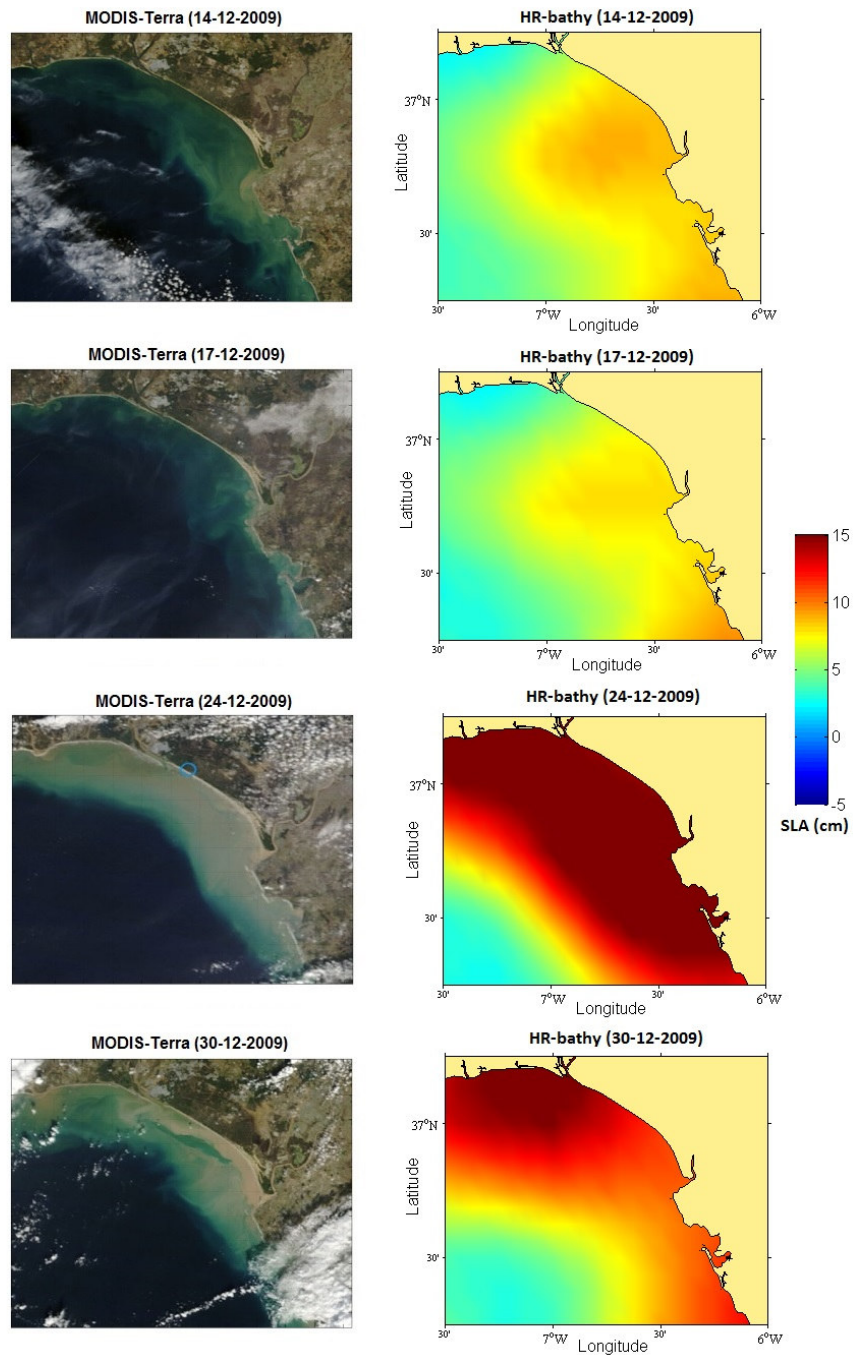


Figure 8. Left panel: RGB MODIS Terra images acquired in several dates during December 2009. Right panel: corresponding HR-bathy maps of SLA.

FIGURE 9

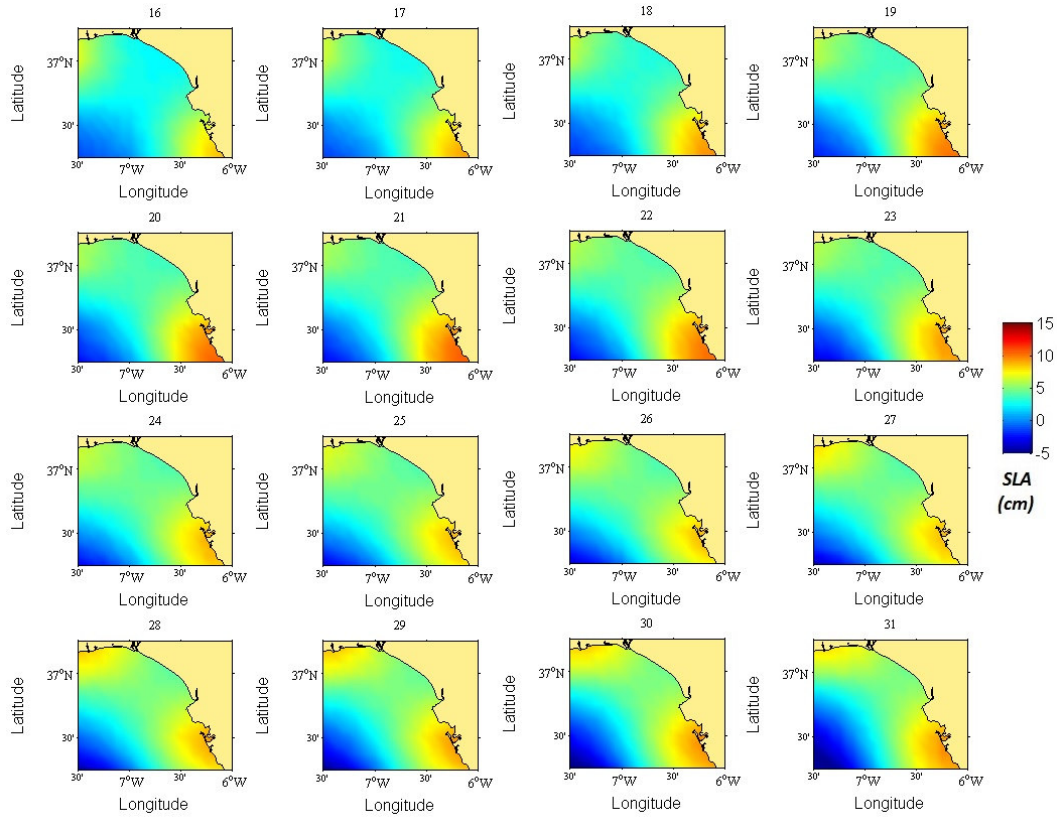
Figure 9. Daily maps of HR-bathy SLA from 16<sup>th</sup> to 31<sup>st</sup> December 1996.

TABLE 1

Table 1. Summary of time periods with heavy river discharge, including the number of days with discharges higher than  $400 \text{ m}^3/\text{s}$  during at least three consecutive days, the maximum discharge in each of the periods and the altimeter missions available.

	Months	Nb. of days	Maximum discharge ( $\text{m}^3/\text{s}$ )	Altimeter missions available
<b>1996</b>	January-February (1)	35	2045	ERS-2 / TP <sup>(1)</sup>
	December (2)	19	3670	
<b>1997</b>	January-February (3)	42	2180	ERS-2 / TP <sup>(1)</sup>
	November-December (4)	24	2800	
<b>1998</b>	January-February (5)	36	1850	ERS-2 / TP <sup>(1)</sup>
<b>1999</b>	October (6)	5	985	ERS-2 / TP <sup>(1)</sup>
<b>2000</b>	December (7)	4	662	ERS-2 / TP <sup>(1)</sup> GFO
<b>2001</b>	January (8)	3	1137	ERS-2 / TP <sup>(1)</sup> GFO
	March (9)	15	2028	
<b>2003</b>	December (10)	7	1000	ERS-2 / TP <sup>(2)</sup> Envisat / GFO / J1 <sup>(1)</sup>
<b>2004</b>	February (11)	4	1235	ERS-2 / TP <sup>(2)</sup> Envisat / GFO / J1 <sup>(1)</sup>
<b>2009</b>	December (12)	10	1579	ERS-2 / J1 <sup>(2)</sup> / J2 <sup>(2)</sup> / Envisat

<sup>(1)</sup> Referenced orbit

<sup>(2)</sup> Interlaced orbit